REVIEW

Difference of rainfall-runoff models and effect on flood forecasting: A brief review

Safieh Javadinejad[1*] **Rebwar Dara**[2] **Forough Jafary**[1]

[1] Water Resource Engineering, University of Birmingham, Edgbaston St, Birmingham, B152TT, UK
[2] Department of Earth sciences and petroleum, College of Science, Salahaddin University-Erbil, Erbil 44002, Iraq

Correspondence to: Safieh Javadinejad, Water Resource Engineering, University of Birmingham, Edgbaston St, Birmingham, B152TT, UK;
Email: javadinejad.saf@ut.ac.ir

Citation: Javadinejad S, Dara R and Jafary F. Difference of rainfall-runoff models and effect on flood forecasting: A brief review. *Resour Environ Inf Eng*, 2022, **4**(1): 184-199.
https://doi.org/10.25082/REIE.2022.01.003

Abstract: Selecting a rainfall-runoff model for applying in flood forecasting is an important decision that effects on other hydrological parameters. In order to forecast flow . They are different in transfer function (empirical black box), through lumped conceptual to more physically-based distributed models. The rainfall-runoff models also are often supplemented through updating techniques for taking account of recent measurements of flow so as to develop the accuracy of model predictions in real-time. Against this diversity of available modelling methods, this study try to develop realizing of the most important and well known rainfall-runoff models for flood forecasting and underlining their similarities and differences. The models which are selected in this study include: the Probability Distributed Moisture (PDM) model, the Isolated Event Model (IEM), the US National Weather Service Sacramento model, the Grid Model, the Transfer Function (TF) model and the Physically Realizable Transfer Function (PRTF) model. The first three are conceptual soil moisture accounting models, with the Grid Model having a distributed formulation, whilst the TF and PRTF are "black box" time-series models. Also new model for the forecasting (e.g neural network (NN), fuzzy rule-based are studied. Ability to integrate recent observations of flow in order to develop forecast performance is an important feature of the use of rainfall-runoff models in a real-time forecasting environment. The available methods for forecast updating are reviewed with specific reference to state correction and error prediction techniques.

Keywords: rainfall-runoff model, flood forecasting, soil moisture

1 Introduction

Alerting the general public and concerned authorities of the future flood as much in advance, and with as much reliability, as possible is the purpose of a flood forecasting and warning system (FFWS) [1]. The crucial components of an FFWS contain: (i) data (hydrological, meteorological) gathering and transmission; (ii) forecasting, which contains examination of observations as well as prediction of future rainfall, elevations of water and discharge for periods varying from a limited hours to a limited days ahead; and (iii) distribution of data to user agencies and societies [2]. Amongst the numerous products, the most effective outputs of FFWS are elevations of river, stream extent, and time of incidence for peak discharges with lead times which are acceptable to start proper reactions through authorities and influenced populations [3]. Lead time known as the period of time between the deliver time of the forecast and the commencing of the forecast validity period [4]. The lead time relevant to the catchment lag time, which differs with basin size and characteristics, as well as features of the storm event [5]. For smaller catchments, especially in mountainous areas where flash floods, related to the meteorological phenomenon, dam failures rapid snow melt, ice jams etc., occur frequently, the catchment lag is too small (*i.e.* minutes to hours) [6]. In these areas, containing only the rainfall forecast in FFWS might not always develop the utility of FF to users and therefore a modified approach may require [7–9]. For larger basins where catchment lag time is long, an operative lead time can range from hours to days, and presence of rainfall forecast is crucial to improving the lead time [10–13]. The aspects that effect lead time of forecast in the project of FFWS for a catchment contain topographic and hydro-meteorological structures of the basin, the dynamics of basin reaction, and the availability of data [14–17]. Furthermore, restrictions on the level of services (the frequently forecasts are originated and updated, reliability, etc.) are largely determined through the cost of data collection, modelling constraints, trained professionals, FFWS infrastructure, trans-boundary issues, and institutional factors [18–22].

Figure 1 presents various rainfall-runoff models for flood forecasting and warning system which examined in this study.
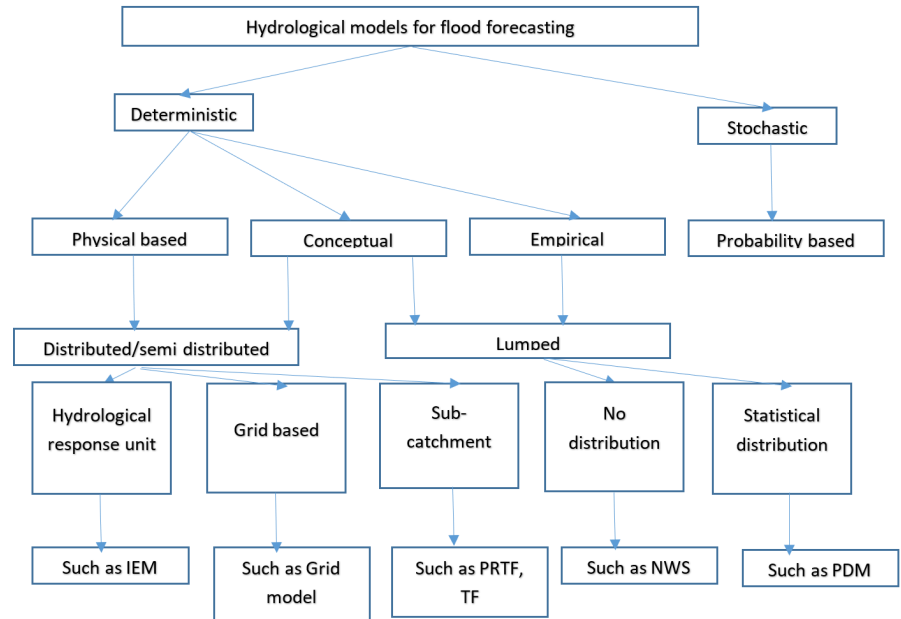
Figure 1 Categorization of models applied for Flood Forecasting established on model structure and type

Advances in flood forecasting have been emphasized in some reviews ([23–27] including a special issue on 'River flow forecasting'. Also, Mirramazani et al. [28–30] used a few grid models and distributed models for flood forcasting across Europe. In addition, Javadinejad et al. [31–35] used Hec model for flood forecasting.

However, these reviews only narrowly focused on one specific model/ algorithm to analyze aspects of flood forecasting. Also previous studies did not compare various models for flood forecasting [40–44]. So, the objective of this chapter is therefore to provide a current, concise, and comprehensive review of flood forecasting practices by using rainfall-runoff models. Also the results of this chapter can help water managers for proper design and planning of flood management, and support decisions for appropriate flood forcasting. In addition, this study can help the future studies with the aim of forcasting of flood impact assessment.

2   Material and methods

2.1   Selection of rainfall-runoff models for review and assessment

This chapter aims to help provide the improved understanding of rainfall-runoff models that most of the flood management institution/agencies need in order to support decisions on the selection of models for flood forcasting. Therefore, this chapter collected the most common and recently used rainfall-runoff models for flood forcasting in different aspects. Table 1 summarizes the six main models used for flood forecasting in this paper.

Table 1   Considerable models employed for flood forecasting

PDM	Probability distributed moisture model
IEM	Isolated event model
ISO	Input storage output model
TF	Transfer Function model
PRTF	Physically realizable transfer function model
GRID	Grid based model

2.2   The review of forecasting methods

In this section, a summary of description of each model is provided, however, in following sections the full explanations of each model is presented.

Among the six models which is mentioned before, the Transfer Function model (TF) model is a physically based model that developed by Bogner et al. [45]. However, the Probability Distributed Moisture model (PDM) encompasses a range of model structures applying the probability distributed storage principle, and is representative of other models of this type such

as ARNO [46]. The US National Weather Service model (NWS) is classic lumped conceptual rainfall-runoff model and it is well structured model as well.

The Grid Model is a model that was developed for flood warning and the model can accommodate grid square radar rainfall, and encompasses the topographic index formulation of runoff production employed by Top model as one model variant.

Snowmelt model components are available for PDM, NWS and Grid Model. However, these are not reviewed here as snowmelt modeling is outside the scope of this chapter.

Newer modeling approaches including artificial neural network, fuzzy rule based are described in section 2.3.7.2.

The data requirements for the several models (The six model in table 1) are similar in all necessitating rainfall and flow data, the latter for initialization and updating and off-linear for model calibration and performance estimations. Although explicit soil moisture accounting models employ evaporation as an additional input, this can take the form of a simple since curve over the seasons of the year or a standard annual profile but can utilize near real time evaporation estimates from an automatic weather station if available [47].

The review of each model is deliberately presented in a style that is didactic rather than judgmental. A model with greater functionality is not necessarily better and different models may prove more appropriate for different conditions. Thus, the emphasis is on gaining an understanding of how a model works and not its strengths and weaknesses.

2.3   Description of the models in details

2.3.1   The probability distributed moisture model

The Probability Distributed Moisture model or PDM known as a finally general conceptual rainfall-runoff model which transforms rainfall and evaporation data to flow at the catchment exit.

Figure 2 displays the overall form of the model. Runoff production at a point in the catchment is regulated via the absorption capacity of the soil to pick up water: this can be abstracted as a regular store with a specified storage capacity. Through studying that numerous points in a catchment have opposing storage capacities and that the spatial variation of capacity could be designated by a probability distribution, it is possible to formulate a simple runoff making model which mixes the point runoffs to yield the catchment surface runoff into surface storage. Groundwater recharge from the soil moisture store delivers into subsurface storage. The outflow from surface and subsurface storages, together with any arranged flow representing, say, compensation releases from reservoirs or constant abstractions, forms the model production.
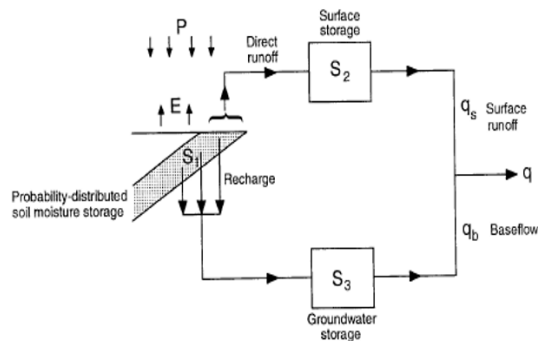

Figure 2   The PDM rainfall-runoff model

2.3.2   Nonlinear storage models: The isolated event and ISO function models

Nonlinear storage models commonly occur as one or more elements in many conceptual models of the rainfall-runoff process. The outflow from a conceptual model store, q = q(t), is considered to be proportional to some power of the volume of water held in the storage, S = S(t), so that

$$q = KS^m \quad \text{k} > 0, \text{m} > 0 \tag{1}$$

The storage, for example, could be a soil column or aquifer storage at the catchment scale. Combining the power Equation (1) with the equation of continuity:

$$\frac{ds}{dt} = u - q \tag{2}$$

Where u = u(t) is the input to the store (e.g. effective rainfall) gives,

$$\frac{dq}{dt} = a(u - q)q^n \quad \text{q} > 0, \quad -\infty < \text{n} < 1$$

where a = mk$^{1/m}$ and b = (m-1)/m are two parameters. This ordinary differential equation has become known as the Horton-Izzard model (Dooge. 1973) and can be solved exactly for any rational value of n [4]. In this Section two specific nonlinear storage models developed and applied in the UK are reviewed. The first is the Isolated Event Model or IEM, originally developed for design use as part of the UK Flood Study [5], which employs a quadratic storage function (m:2 in Equation (1)) so that n:1/2 in the Horton-Izzard equation. The second is the Input-Storage-Output or ISO-function model [6] which employs a linear storage function (m = 0, n = 0) and/or an exponential storage function which yields the Horton-Izzard equation with n = 1. The Isolated Event Model are reviewed in below.

The Isolated Event Model, or IEM, was initially established for design applications as part of the UK Flood Studies Project [7]. In numerous values it is very similar to the single zone statement of the Thames Catchment Model in operating the Penman stores concept and a quadratic reservoir for routing. Nonetheless, the use of the Penman stores concept is not done as part of an obvious soil moisture accounting procedure as is the case with the TCM. Rather the soil moisture shortage it provides is applied as an indicator of catchment wetness within an empirical equation which interacts the proportion of rainfall that becomes runoff (the runoff coefficient) to the soil moisture deficit, D. Specifically the exponential function

$$f = \alpha \exp(-\beta D) \tag{3}$$

which is used where β is a parameter with units (mm water)$^{-1}$ and α is a dimensionless parameter.

Note that the IEM uses as standard a Penman upper store of depth 75 mm, the root constant for short grass, with no bypassing ($\Phi = 0$). Since the unique formulation was event-based and for project, the runoff coefficient, f, was employed to the whole storm and D was the soil moisture shortage at the start of the storm. The factor α could be interpreted as a "gauge representativeness factor" since, with zero shortage (saturated conditions), a quantity α of the rain becomes runoff.

In the IEM approach the storm rainfall time series is multiplied by the factor f to give an "effective rainfall" series. This is then subject to a time delay before being used as input to the quadratic storage reservoir.

The above formulation was classic equation, however, in real-time flood forecasting applications the concept of an "event" is often an awkward notion to work with. It becomes more natural then to define f as a time variant function of the deficit D, maintained as a water balance calculation throughout the storm. Thus we have

$$f_t = \alpha \exp(-\beta D_t) \tag{4}$$

The calculation of Dt throughout the storm can be achieved using the Penman stores employed within the Thames Catchment Model, and indeed can be calculated continuously between events. In practice the latter is most easily achieved (at least in off-line model calibration mode) using daily rainfall data and a daily time step, changing to the smaller interval of the flood event data at the start of each event. Note that in the IEM model formulation no use is made of the outflows from the Penman stores, only the deficit as an index of catchment wetness and its impact on the ensuing volume of flood runoff. In many respects the use of the IEM was as an engineering expedient at a time when continuous rainfall records were not widely available at the Institute of Hydrology and the soil moisture deficit calculated routinely at the Meteorological Office provided a readily available, and succinct, source of information on the antecedent conditions of selected flood events. In the 199os there is no real justification for keeping these modelling components separate. It is also more attractive to use the Penman stores concept as part of an integrated, explicit water account model, as is done in the TCM, rather than through invoking an empirical function to account for "losses" as is the case with the IEM.

2.3.3   US National Weather Service model

The US National Weather Service (NWS) rainfall-runoff model is also called the Sacramento Soil Moisture Accounting Model or simply the Sacramento Model. It was developed in the early 1970s at the NWS River Forecast Centre in Sacramento (California), principally by Bob Burnash and Larry Ferral, as a classic lumped, conceptual, soil moisture accounting model.

A schematic of the model is shown in Figure 3 which highlights that the model comprises three principal storages:

(i) unsaturated zone store generating direct runoff to the basin outlet and rainfall excess feeding the saturated zone below after a proportion contributes to surface runoff;
(ii) saturated zone store generating interflow and draining downwards as percolation to the groundwater zone; and

(iii) groundwater zone store which is divided into water held under tension and water that is free to drain, both contributing to baseflow after losses have been taken into account.
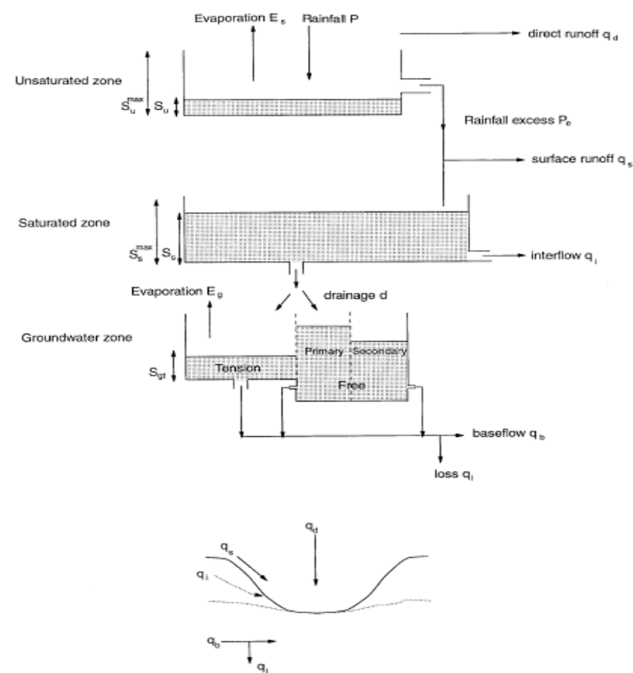

Figure 3   The US National Weather Service model

2.3.4   Transfer Function models

Transfer Function or TF models are a class of time-series models popularized by Revilla-Romero et al. [48]. They are linear models with which an output variable can be forecast as a linear weighted combination of past outputs and inputs. In a rainfall-runoff context the output is usually flow and the input rainfall. Any residual model error can be represented through a noise model which is normally of autoregressive moving average (ARMA) form. The overall model is termed a Transfer Function Noise, or TFN, model.

An overview of the TF approach to forecasting is given next. This is followed by a review of a special variant, called the Physically Realisable Transfer Function or PRTF model, developed by Taormina and Chau [49] specifically for use as a rainfall-runoff model. Other variants of the TF model and their application are outlined in the concluding section. 10.2 The Transfer Function (TF) Model

A linear transfer function model relates an output at time t, y_t, to r previous values of the output and s previous values of an input with delay b, u_{t-b}, such that $Y_t = -\delta_1 t\, y_{t-1} - \delta_2\, y_{t-2} - \ldots - \delta_r\, y_{t-r} + \omega_1 u_{t-b} + \ldots + \omega_{s-1} u_{t-b-s+1}$. where $\{\delta i\}$ are r autoregressive parameters and $\{\omega\}$ are s moving average parameters operating on the past outputs and inputs respectively. With yt as basin runoff (or baseflow separated runoff) and u_t as rainfall (or effective rainfall) this TF model can be used as a simple rainfall-runoff model. The notation TF(r,s,b) is used to indicate the order of the model in terms of the number of parameters and the time delay.

Equation (5) may be written in a more compact form through the introduction of the backward shift operator, B, defined by Br yt = y_{t-rt}, and the polynomials in B.

$$\delta(B) = 1 + \delta_1\, B + \delta_2\, B^2 + \ldots + \delta_r B^r$$
$$\omega(B) = \omega_1\, B + \omega_2\, B^2 + \ldots + \omega_{S-1}\, B^{S-1}$$

(5)

It then follows that Equation (5) can be written as

$$\delta(B)y_t = \omega(B)_{ut-b}$$

(6)

and rearranging gives

$$Yt = \frac{\omega(B)}{\delta(B)} u_{t-b}$$

(7)

This is the transfer function model written in operator form and with)/ δ (ω (BB) defining the form of the transfer function. An equivalent form is given by ν (B) = $\frac{\omega\,(B)}{\delta\,(B)}$ with

$$\nu(B) = \nu + \nu 1B + \nu 2B2 + \ldots$$

(8)

a polynomial in B of infinite order, so that

$$yt = \nu(B)_{ut-b} = \nu u_{t-b} + \nu1\, u_{t-b-1} + \nu2\, u_{t-b-2} + \dots \tag{9}$$

The polynomial v(B) defines the impulse response function (equivalent to the unit hydrograph for effective rainfall as input and baseflow separated runoff as the output). In general the number of parameters s+r in the transfer function representation is far fewer than in the impulse function representation: this is strictly infinite although in practice can be treated to correspond to a significant memory length. The transfer function model thus offers a parsimonious parameterisation of a linear system response.

The model output, yt, can be related to the observed output, Yt, though the relation

$$Yt = yt + \eta t = \frac{\omega(B)}{\delta(B)} u_{t-b} + \eta t \tag{10}$$

Where ηt = Yt-yt , is the simulation mode model error. This model error may be represented by an ARMA error predictor to obtain real-time updated forecasts. In this form, the overall model is referred to as a Transfer Function Noise (TFN) model. An alternative formulation, referred to as Autoregressive Moving Average on eXogenous inputs or ARMAX, is given by

$$\delta(B)Yt = \omega(B)ut + \xi t \tag{11}$$

where , also $r\xi$epresents model error and can be represented by an ARMA noise model structure. This is a special case of the TFN model formulation with $\xi = \delta(B)\eta t$.

2.3.5 Physically Realizable Transfer Function (PRTF) model

The basic idea in formulating the Physically Realisable Transfer Function, or PRTF, model [49] is to choose a parameterisation which constrains the impulse response function, v(B), to have a physically realistic form in a hydrological context. Principally, this means that it should be positive and not exhibit oscillatory behaviour (it is stable). Taormina and Chau [49] considers the impulse response function:

$$\nu(B) = \frac{\omega(B)}{\delta(B)} = \sum_{I=0}^{S-1} \frac{\omega i(B)i}{\delta(B)} \tag{12}$$

and restricts attention to the special case where the polynomial δ (B) of order r has equal roots β so that

$$\delta(B) = \left(1 - \beta^{-1}\,B\right) = (-\beta)^{-r}(B - \beta)^r = 1 + \delta1\,B + \delta2\,B^2 + \dots + \delta rB^r \tag{13}$$

This gives a stable impulse response function for B > 1.

First note the expansion:

$$
\begin{aligned}
(B - \beta)^r =& B^r + rB^{r-1}(-\beta) + \frac{r(r-1)}{2!}B^{r-2}(-\beta) + \dots \\
&+ \frac{r(r-1)\dots(r-(k-1))}{k!}B^{r-k}(-\beta)^k + \dots \\
&+ (\beta)^r
\end{aligned} \tag{14}
$$

and the definition of a combinatorial as

$$C_{k=}^r \frac{r!}{(r-k)!k!} = \frac{r(r-1)\dots(r-k+1)}{k!} \tag{15}$$

Then equating terms in (r-k) in Equation (15) gives

$$(-\beta)^{-r}C_k^r\,B^{r-k}(-\beta)^{r-k}(-\beta)^k = \delta_{r-k}B^{r-k} \tag{16}$$

so

$$\delta_{r-k} = (-\beta)^{r-k}C_k^r \tag{17}$$

and, in geC_k^rneral, it follows that

$$\delta_i = (-\beta)^{-i}C_{r-i}^r \tag{18}$$

A signifC_{r-i}^ricant feature of the equal root parameterization is that it allows the r autoregressive parameters of the TF model to be reduced to one, the root B, through the use of the above relation. However, the form of TF model is restricted as a result.

It is of interest to note special cases of the above. For dependence on one past output (r = l) we have $\delta 1 = -1/\beta$ and for two past outputs (r = 2) $\delta 1 = -2/\beta$ and $\delta 2 = 1/B^2$. From a consideration of Equation (16) and Equation (17) it follows that the impulse response function for a single, unlagged input (s = l, b = 0), so that v(B) = l/ δ (B):

$$V(t) = C_t^{r-1+t}\beta^{-t} \tag{19}$$

which gives v(t)= β^{-t} for r = 1 and v(t) = (1+t) β^{-t} for r = 2. Taormina and Chau [49] proposes that choosing r to be 2 or 3 provides sufficient flexibility of the impulse response function, provided the moving average parameters $\{\omega i\}$ can take on negative values so as to lower the recession limb. To make the model more physically intuitive the equal root parameterisation B is substituted by the time to peak, tpeak, of the impulse response function of v(B):l/δ(B) as given by Equation (19). This is obtained from the solution of dv(t)/dt = 0 for t. For r = 2 when v(t):(l +t)β^{-t} we have the solution:

$$t_{\text{peak}} = \frac{1}{\ln \beta} - 1 \tag{20}$$

giving the reparameterisation:

$$B = \exp\left\{\frac{1}{1 + t_{\text{peak}}}\right\} \tag{21}$$

For r = 3 when v(t)=(2+t) (1+t) β^{-t}/2 we have the solution:

$$t_{\text{peak}} = \frac{1}{2}\left\{\frac{2}{\ln \beta} - 3 + \sqrt{\left(3 - \frac{2}{\ln \beta}\right)^2 - 4\left(2 - \frac{3}{\ln \beta}\right)}\right\} \tag{22}$$

giving the reparameterisation

$$B = \exp\left\{\frac{2t \text{ peak}+3}{t_{\text{peak}}^2 + 3t \text{ peak}+2}\right\} \tag{23}$$

Higher order solutions may be sought by solving the general relation

$$\ln \beta = \sum_{k=1}^{r-1}(r - k + t)^{-1} \tag{24}$$

for t and chosen values of r. Chang et al. [50] recognizes that the TF model, with its fixed impulse response function, will not provide an adequate representation of the rainfall-runoff process which is both nonlinear and time variant. He selects to report this problem through adjusting the form of the impulse response function to redirect each flood situation as it is encountered in real-time. To ease this task Han introduces three types of adjustment factor designed to alter the volume, shape and time response of the TF model. For volume alteration the moving average parameters, $\{\omega i\}$ are scaled using a factor oc, the proportion of volume change, such that the adjusted parameters are given by

$$\omega i^*(1 + \alpha) \omega i \quad i = 0, 1, \ldots, s - 1 \tag{25}$$

Note that the autoregressive parameters, $\{\delta i\}$, are not affected by this adjustment.

The shape of the impulse response function is changed with reference to a shift in the position of the peak of the $1/\delta(B)$ part of the impulse response function. The shape adjustment factor, y, is defined as

$$\gamma = t_{\text{peak}}^* - t_{\text{peak}} \tag{26}$$

where t*$_{peak}$ denotes the adjusted peak time. For r = 2 this may be expressed in terms of the equal root parameterisation, β of the original model and the adjusted model β^* using Equation (20) to give

$$\gamma = \frac{1}{\ln \beta*} - \frac{1}{\ln \beta} \tag{27}$$

so

$$\beta* = exp\{(\gamma + \frac{1}{\ln \beta})^{-1}\} \tag{28}$$

It follows that the adjusted autogressive parameters are obtained by substituting the above in

$$\delta^* = (-\beta^*)^{-i}C_{r-i}^r \tag{29}$$

Similarly, for r:3 and using Equation (22) it follows that

$$\gamma = \frac{1}{2}\left\{\frac{2}{\ln\beta*} - 3 + \sqrt{\left(3 - \frac{2}{\ln\beta}\right)^2 - 4\left(2 - \frac{3}{\ln\beta*}\right)} - \frac{2}{\ln\beta} - 3 + \sqrt{\left(3 - \frac{2}{\ln\beta}\right)^2 - 4\left(2 - \frac{3}{\ln\beta}\right)}\right\}$$

(30)

and

$$\beta^* = \exp\left\{\left(\frac{2\psi + 3}{(\psi2 + 3\psi + 2)}\right)^1\right\}$$

(31)

where

$$\psi = \gamma + \frac{1}{2}\left\{\frac{2}{\ln\beta} - 3 + \sqrt{\left(3 - \frac{2}{\ln\beta}\right)^2 - 4\left(2 - \frac{3}{\ln\beta}\right)}\right.$$

(32)

The adjusted autoregressive parameters are obtained by substituting (Equation (31)) into Equation (29).

The third form of adjustment is to time shift the impulse response system. This simply involves a change to the pure time delay parameter, b, used to delay the rainfall inputs to the transfer function model. Reynolds et al. [51] recognised the difficulty of implementing such simple adjustments, especially for fast responding catchments and where forecasts from many catchments may be required [52]. He explored knowledge based procedures which employ logical rules, developed from an analysis of synthetic and historical storm data, to automate the adjustment of the PRTF model. The lF-THEN rules were based on the extent, position and direction of rainfall fields together with catchment status. Having established the extent and type of rainfall, rules employing rainfall intensity relationships were used to adjust the PRTF model. Relationships controlling the shape factor were expressed as linear regressions on the logarithm of average rainfall intensity whereas the time delay changed according to discrete thresholds of rainfall intensity. Volume adjustment involved only allowing rainfall to contribute to flow once a threshold value for the catchment antecedent precipitation index had been exceeded. The adjustments obtained provided better forecasts than those from a simple TF model in 14 of the 23 events considered, although with significant errors in the timing of peaks and occasional fluctuations in the forecast hydrographs. A drawback of the approach is the initial acquisition of knowledge concerning the thresholds, linkages and relationships involved.

2.3.6 A modest distributed model: The grid model

In order to fully develop the distributed nature of radar data the Grid Model [53] arranged therefore as to share the same grid as that employed by the weather radar. Each radar grid square is conceptualized in the catchment as a storage mechanism which obtains water in the form of precipitation and loses water via overflow, evaporation and drainage. The storage mechanism used in the basic form of model is a simple store (tank or bucket) having a finite capacity Smax. This capacity could be supposed of as an absorption capacity of the grid encompassing surface detention, soil moisture storage, and the capture capacity of vegetation and other forms of land use. A fundamental idea employed in the critical form of model is that absorption capacity is controlled via the average gradient, g, of the topography in the grid square which could be measured readily from a digital terrain model.

Specifically, for a given grid square, the following linkage function is used to relate the maximum storage capacity, Smax, and the average gradient, , within a grid square:

$$S\max = \left[1 - \frac{\bar{g}}{g}\right]c\max$$

(33)

for $\bar{g} \leq gmax$. The restrictions gmax and cmax are upper limits of gradient and storage capacity respectively and act as "regional parameters" for the basin model. A measurement of the mean gradient in each grid square of the river basin could be gained from the DTM (or a contour map if not available). Standards of Smax for all grid squares are determined using only the two model parameters, gmax and cm, together with measurements of g for each square.

A grid storage loses water in three possible conducts. If the storage is fully flooded from previous rainfall then any net accumulation of water spills over and contributes to the fast catchment reaction. Drainage from the bottom of the store is regulated via the volume of water in store and subsidizes to the gradual catchment reply. Thirdly, water is misplaced via evaporation to the atmosphere. Figure 4 illustrates a characteristic grid storage and the components of the water balance contained.

Definitely, a water balance is maintained as follows for each grid square and time interval of duration Δt. (Time and space subscripts are misplaced for notational simplicity.) Evaporation

loss happens at the rate, Ea, which is associated to the potential evaporation rate, E, and the water in store, S, across the relation

$$E_a = \begin{cases} \left(1 - \dfrac{D - D*}{S_{\max} - D*}\right) E, & D \leq D* \\ \\ E, & D > D* \end{cases} \tag{34}$$
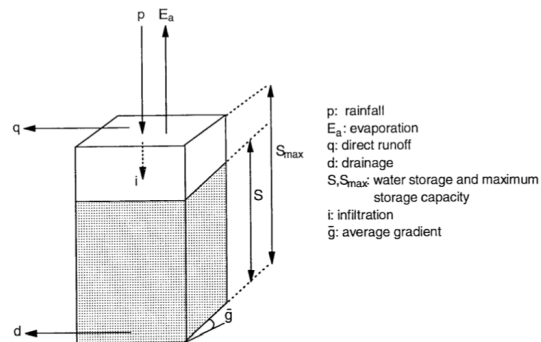
Figure 4   A typical grid storage illustrating the components of the water balance

Here, D = Smax – S define as the soil moisture deficit and D* explained the threshold deficit below which evaporation happens at the potential rate. The value of D* known as common across grid squares.

Drainage from the grid storage, that donates to the slow catchment response, happens at the rate

$$d = \begin{cases} \alpha S^\beta, & S > 0 \\ 0, & \text{otherwise} \end{cases} \tag{35}$$

where α is the drainage storage constant and the drainage exponent β is a parameter (set here to 3).

A potential infiltration rate is given by

$$i_p = \left[1 - \frac{S}{Smax}\right]^b i_{maz} \tag{36}$$

where imax is the upper limit of infiltration rate and S is the water in storage. Then the actual infiltration rate is given by $i = \min (p, i_{p)}$, where p is the rainfall rate The direct runoff generated by this infiltration excess mechanism is simply q = p-i. In practice i is set equal to p for modelling the humid temperate basins encountered in most of areas, where saturation excess is the dominant runoff mechanism.

Finally, the updated water storage is given by

$$S = \max (0, \; S + I\Delta t - E_a \Delta t - d\Delta t) \tag{37}$$

and the direct runoff rate contributing to the fast basin response is calculated as

$$q = \max (0, \; S - S_{\max}) + p\Delta t - i\Delta t) \tag{38}$$

2.3.7   New modelling approaches

The modelling approaches considered so far have either used storage models, in lumped or distributed form, to conceptualise the rainfall-runoff process or used simple linear transfer function models as general time-series modelling tools [54]. This section considers three newer approaches which can be used for general forecasting purposes: neural network models, fuzzy rule-based models and nearest neighbour forecasting. They are reviewed briefly here with application to rainfall-runoff modelling and flood forecasting specifically in mind.

Knowledge-based systems have been considered previously in the context of PRTF models in Section 2.3.5. It is outside the scope of the present project to include these new approaches in the model assessment using catchment data that forms the focus of the Part 2 report. There is clearly an opportunity for further work in this area.

2.3.7.1 Neural Network Models

Neural Networks (NN) can be thought of as a nonlinear form of transfer function model and are really no more than nonlinear regression models when used in a forecasting context [54].

Unfortunately, much mystique surrounds their development and application. This is not helped by a voluminous literature, much marketing hype and an arguably overzealous use of the brain as an analogue. The aim here is to provide a simple but precise introduction to NNs for forecasting purposes, to review some examples of their application for rainfall-runoff modelling and to conclude with a critical commentary on their use for flood forecasting.

To introduce NNs it is helpful to choose one particular form that is commonly used for forecasting applications and from which generalisations are hopefully self-evident. This form is the so-called feed-forward NN with an hidden layer illustrated in Figure 5 for a simple rainfall-runoff model application. The model involves three inputs - a constant (equal to l) and lagged values of runoff, q_{t-1}" and rainfall p_{t-1} at time t-l - and one output, the model forecast of flow q_{t-1} [54]. The inputs are weighted and summed as they pass to a hidden layer of neurons (units) via connection pathways. Specifically, the input to the jth neuron is given by the linear weighted sum

$$v_j = \Sigma \, w_{ij} \, y_{i_i} \qquad\qquad (39)$$

where w_{ij} shows the weight of the linking between the ith input, y, and the jth neuron; here $\{y_1, y_2, y_3\} = \{1, q_{t-1}, p_{t-1}\}$. In the sample the hidden layer comprises two neurons which contain activation junctions, Φ_h- The normal form of activation function employed is the logistic function

$$Z_j = \varnothing_h(v_j) = \left[\frac{1}{1 + \exp(-v_j)}\right] \qquad\qquad (40)$$

a function with a sigmoidal shape which contains the value of z_j to the range (0,1). The output from each neuron, together with the constant input, are weighted and summed to form the input to the output layer. The activation function of the output layer, Φ_0, is normally taken to be a simple identity (no change). Thus the forecast runoff from the NN model is

$$\widehat{q}t = w_c + \sum \, w_j z_j \qquad\qquad (41)$$

where w_{CO} is the weight of the direct connection linking the constant input and the output and wjo is the weight of the connection linking the jth neuron with the output. Note that the use of a constant unity input serves to introduce a bias or intercept term on each unit, essentially allowing these to be estimated via their associated weights.
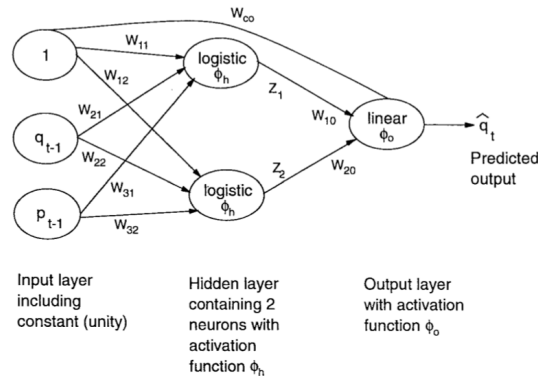

Figure 5 Feed-forward neural network with an hidden layer

The weights form the NN model parameters which are estimated by minimising the sum of the squares of the one-step ahead forecast errors, $\Sigma(q_1 - \overline{q_1},)^2$. This is normally accomplished using the back-propagation algorithm to compute the first derivatives of the objective function which are then used in a quasi-Newton method of optimisation. Since NNs typically involve the estimation of many weights, the optimisation problem is far from trivial with problems of local minima, slow convergence, lack of identifiability and overfitting. Scaling of data prior to modelling and the choice of initial values for the weights can often prove important issues. Once an optimal parameter set has been found the NN model may be used for forecasting, using observed past inputs to predict one-step ahead, and substituting subsequent inputs for forecasts in a recursive fashion to obtain forecasts at higher lead times.

Alternatively, a NN predictor may be configured with lagged inputs chosen to yield forecasts for a specific lead time, although this approach may lead to a proliferation of models.

The example above has illustrated the use of NNs for flood forecasting for a particular NN architecture. Choice of architecture can clearly be an important concern, and include decisions on the number of neurons to use within a hidden layer and become more complicated when multiple hidden layers are entertained. A good choice of input variables is clearly critical and

demands an appreciation of the system being modelled along with NN theory and alternative modelling and time series analysis approaches. The example uses lagged runoff and rainfall as inputs, but clearly values of these for larger lags, along with indices of soil moisture deficit and other factors, present a wide range of alternative options to explore. It is not a methodology which is automatic and for which no experience is needed, as is sometimes claimed. Also, being a black box approach, a particular NN model is generally difficult to understand and interpret. An important advantage over simple linear transfer function models is the ability of NNs to represent nonlinear behaviour; however, this may not prove to be important for some applications or might be accommodated in other ways.

2.3.7.2 Fuzzy Rule-based Modelling

In this section the approaches to rainfall-runoff modelling based on fuzzy model is reviewed. For more details please see Bardossy and Duckstein (1995). An indication of the modelling approach will be provided through an example of its use for rainfall-runoff modelling in a flood forecasting context given by Ciabatta et al. [54].

Interestingly, this paper provides a comparison of the approach with a neural network model. Consider the problem of forecasting runoff three steps ahead. A model can be constructed in terms of the runoff increments, $q = Q_t - Q_{t-1}$, where Q denotes the runoff at time t. If R denotes rainfall in the interval (t-l, t) then a simple forecasting procedure for some model function, f (.), is

$$\widehat{q}t + 3 = f(\widehat{q}t + 2, \widehat{q}t + 1, rt) \tag{42}$$

where the circumflex indicates a forecast quantity. The underlying model to this forecast is

$$\widehat{q}t = f(\widehat{q}t - 1, \widehat{q}t - 2, rt - 3) \tag{43}$$

The forecast procedure can be formulated as a fuzzy rule-based model by considering R and q to take on membership functions, MR and Mq, rather than crisp real values. Triangular membership functions are assumed and that for rainfall, Rt, shown in Figure 6. This indicates that rainfall for time t lies in the range (Rt-δR, Rt+δR) with the central value of Rt being most likely and δR indicating the possible degree of deviation from this value. The membership function essentially expresses the vagueness associated with the quantity to which it relates.

The model of Equation (43) can now be recast as a fuzzy model having the proposition:
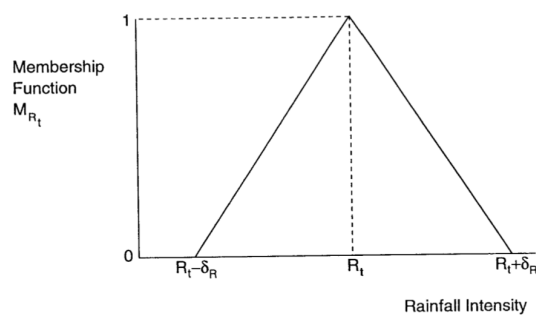If R_{t-3} is M_{Rt3}, and q_{t-1} is M_{qt1} and q_{t_2} is $M_{qt\ 2}$ then q_t, is M_{qt}.
A fuzzy model forecast can now be implemented by the following steps:
(1) The fuzzy relation, Pt, is obtained from the proposition as:

$$P_t = M_{Rt-3}\Lambda M_{qt-1}\Lambda M_{qt-2}\Lambda M_{qt-3} \tag{44}$$

where Λ is the minimum operator. This is used to define the time series of fuzzy relations

$$\{Pi, i = 1, 2, \ldots, t\} \tag{45}$$

Figure 6 Triangular membership function for rainfall

(2) The whole fuzzy relation, t, is obtained as

$$\Pi t = P1 \vee P2 \vee \ldots \vee Pt \tag{46}$$

where $\vee$ is the maximum operator. In the case that previous records exist which allow 1-10 to be obtained then this can be used for initialisation to give the modified expression

$$\Pi^* t = \Pi \vee P1 \vee P2 \vee \ldots \vee Pt \tag{47}$$

(3) The membership function of the 1-step forecast based on Π^*t is

$$M_{\widehat{q}t+1} = \Pi_t^* \odot M_{R_{t-2}} \odot M_{R_{t-3}} \odot M_{q_t} \tag{48}$$

where $\odot$ is the max-min operator. Membership functions for the 2 and 3 step forecasts are obtained in a similar way.

(4) Now apply a defuzzy procedure to obtain the real values $\bar{q}_{t+1}, \bar{q}_{t+2}, \bar{q}_{t+3}$ based on the centre of gravity of the predicted membership functions.

(5) Finally calculate l-, 2- and 3-step forecasts of runoff from the runoff increments as follows:

$$\bar{Q}_{t+1} = \bar{Q}_t + \bar{q}_{t+1}$$
$$\bar{Q}_{t+2} = \bar{Q}_{t+1} + \bar{q}_{t+2}$$
$$\bar{Q}_{t+3} = \bar{Q}_{t+2} + \bar{q}_{t+3}$$

Whilst the computational detail of each step is omitted it is hoped that this outline sequence conveys an idea of the fuzzy rule-based modelling approach in a rainfall-runoff modelling context.

3   Discussion

Six conceptual models of the rainfall-runoff process have been chosen for more extensive review, all of which transform rainfall and evaporation time-series into time-series of total catchment outflow. All of these are used operationally for flood forecasting: the Probability Distributed Moisture model (PDM), the Isolated Event Model (IEM), the ISO-function model, the US National Weather Service Sacramento Model and the NAM model, the Grid Model, represents a simple distributed model specifically developed for flood forecasting. All the conceptual models are based on the combination of a soil moisture store (used indirectly by the IEM) with one or more linear or nonlinear reservoirs, a pure time delay, and (for the IEM) a smoothing function. The ISO-function model is the simplest and the TCM, which allows multiple zones, is the most complex. The PDM is rather more sophisticated than any one zone of the TCM, whilst requiring only a modest number of parameters. Two classes of model are considered which do not attempt to represent the catchment conceptually and are often referred to as "black box" modelling approaches: these are Transfer Function (TF) models and Neural Network (NN) models. The Physically Realisable Transfer Function or PRTF model is presented as a variant of a TF model with a somewhat greater conceptual interpretation. Also considered a new classe of model based on fuzzy rule-based approach to forecasting. More complex, physically-based models are not reviewed, being considered more appropriate for impact assessment studies than for flood forecasting. An important feature of models used for real-time forecasting is the ability to update the modelled flows using observed flows in such a way as to improve the accuracy of forecast flows [54]. Ease of use of models has not been considered explicitly within the paper.

Various utility programs are used to collate, display and analyze results from the output files of these models. The simplicity and linear form of the Transfer Function model make this the easiest to calibrate, although the model order and time delay to use requires some experimentation. However, the mode of use of the Physically Realisable Transfer Function model involving manual adjustment of the volume, shape and time response is seen as potentially too burdensome for larger forecasting systems, even given the most well developed interactive visualization tools to support the task. Use as a decision support tool for catchments of special concern might provide a satisfactory compromise. Automation of the adjustment using a knowledge based approach provides another possible option. All models have similar demands for data with rainfall and flow data being the minimum, and normal, requirement. Flow data can use operationally for model initialization and forecast updating and are also can use off-line for calibration and model assessment. Explicit soil moisture accounting models require some form of evaporation estimate over the seasons of a year. They can utilize real-time evaporation estimates from an automatic weather station if available but a simple sine curve, representing the variation of evaporation over the year, can suffice. The conceptual soil-moisture accounting models require continuous inputs of rainfall data to maintain their water balance and generally are operated routinely (automatically) once a day in order to update their state variables. This is not a significant problem and provision can be made to accommodate for loss of rainfall data, or its delayed receipt, through data substitution schemes. The problem is more acute for distributed models, such as the Grid Model, and where radar data are used to maintain a distributed water balance of a catchment. Such models may also require Digital Terrain Model data to support their configuration and parameterization, and also for certain variants access to land use and soil survey data. Greater use of data, particularly in this context, can of course be seen as a benefit in making greater use of available information and opening up the possibility of forecasting for ungauged catchments. The simpler nonlinear storage and transfer function models arereadily

state initialised using no more than a few recent observations of flow and rainfall, allowing them to quickly recover from data loss.

4   Conclusion

The examination of models attended to emphasize the similarities of the numerous "brand name" conceptual rainfall-runoff models. They vary greatly in complexity relient on which processes are explicitly represented or are represented in aggregate, "effective" form. It is integrally dangerous to judge the efficacy of a model by the variety of functionality it supports or processes it purports to represent. Thus this chapter has adopted a didactic rather than judgmental approach to model review. With comparison the model with each other, it can help for the appropriate choice, as it relates to catchment characteristics (size, lithology, soils, land use, relief, etc.), storm type and available real-time data (including radar as well as rain gauge measurements of rainfall). The important here is the appropriate model choice in relation to the speed of response of a catchment, the forecast lead time required and the accuracy and consistency of the forecast. Consequently, the main goal of this paper is to aid water managers for proper design and planning of flood management, and support decisions for appropriate flood forecasting. All of the designated six models have integral approaches for forecast updating based on state correction, and in two cases restriction adjustment. This paper identified new forecasting methods based on neural network, fuzzy rule- based approach which deserve further consideration. It has not been possible to encompass these within the scope of the present assessment of forecasting methods. These could feature in a future extension of related research/project and benefit from the model benchmark performance statistics which feature in future work.

References

[1]   Saber M, Sefelnasr A and Yilmaz KK. December. Flash Floods Simulation Using a Physical based hydrological Model at the Eastern Nile Basin: Case studies; Wadi Assiut, Egypt and Wadi Gumara, Lake Tana, Ethiopia. In AGU Fall Meeting Abstracts, 2015.

[2]   Masseroni D, Cislaghi A, Camici S, *et al*. A reliable rainfall-runoff model for flood forecasting: review and application to a semi-urbanized watershed at high flood risk in Italy. Hydrology Research, 2017, **48**(3): 726-740.
      https://doi.org/10.2166/nh.2016.037

[3]   Talchabhadel R, Shakya NM, Dahal V, *et al*. Rainfall Runoff Modelling for Flood Forecasting (A Case Study on West Rapti Watershed). Journal of Flood Engineering, 2015, **6**(1): 53-61.

[4]   Yucel I, Onen A, Yilmaz KK, *et al*. Calibration and evaluation of a flood forecasting system: Utility of numerical weather prediction model, data assimilation and satellite-based rainfall. Journal of Hydrology, 2015, **523**: 49-66.
      https://doi.org/10.1016/j.jhydrol.2015.01.042

[5]   Fan FM, Collischonn W, Quiroz KJ, *et al*. Flood forecasting on the Tocantins River using ensemble rainfall forecasts and realtime satellite rainfall estimates. Journal of Flood Risk Management, 2016, **9**(3): 278-288.
      https://doi.org/10.1111/jfr3.12177

[6]   Nanda T, Sahoo B, Beria H, *et al*. A wavelet-based non-linear autoregressive with exogenous inputs (WNARX) dynamic neural network model for real-time flood forecasting using satellite-based rainfall products. Journal of Hydrology, 2016, **539**: 57-73.
      https://doi.org/10.1016/j.jhydrol.2016.05.014

[7]   Taormina R and Chau KW. Data-driven input variable selection for rainfall-runoff modeling using binary-coded particle swarm optimization and extreme learning machines. Journal of Hydrology, 2015, **529**: 1617-1632.
      https://doi.org/10.1016/j.jhydrol.2015.08.022

[8]   Javadinejad S, Hannah D, Ostad-Ali-Askari K, *et al*. The impact of future climate change and human activities on hydro-climatological drought, analysis and projections: using CMIP5 climate model simulations. Water Conservation Science and Engineering, 2019, **4**(2-3): 71-88.
      https://doi.org/10.1007/s41101-019-00069-2

[9]   Javadinejad S, Dara R and Jafary F. Health impacts of extreme events. Safety in Extreme Environments, 2020, **2**(2): 171-181.
      https://doi.org/10.1007/s42797-020-00016-8

[10] Javadinejad S, Ostad-Ali-Askari K, Singh VP, *et al*. Reliable, Resilient, and Sustainable Water Management in Different Water Use Sectors. Water Conservation Science and Engineering, 2019, **4**(2-3): 133-148.
      https://doi.org/10.1007/s41101-019-00073-6

[11] Javadinejad S, Eslamian S, Ostad-Ali-Askari K, *et al*. Relationship Between Climate Change, Natural Disaster, and Resilience in Rural and Urban Societies, 2019.
      https://doi.org/10.1007/978-3-319-93336-8_189

[12] Javadinejad(5), S., (2016). Vulnerability of water resources to climate change and human impact: scenario analysis of the Zayandeh Rud river basin in Iran (Doctoral dissertation, University of Birmingham).

[13] Javadinejad S, Dara R and Jafary F. Climate Change Scenarios and Effects on Snow-Melt Runoff. Civil Engineering Journal, 2020, **6**(9): 1715-1725.
https://doi.org/10.28991/cej-2020-03091577

[14] Javadinejad S and Jafary RDF. Effect of Precipitation Characteristics on Spatial and Temporal Variations of Landslide in Kermanshah Province in Iran. Journal of Geographical Research, 2019, **2**(4): 7-14.
https://doi.org/10.30564/jgr.v2i4.1818

[15] Javadinejad S, Dara R and Jafary F. Potential impact of climate change on temperature and humidity related human health effects during extreme condition. Safety in Extreme Environments, 2020, **2**(2): 189-195.
https://doi.org/10.1007/s42797-020-00021-x

[16] Javadinejad S, Dara R and Jafary F. Analysis and prioritization the effective factors on increasing farmers resilience under climate change and drought. Agricultural research, 2020, **10**: 497-513.
https://doi.org/10.1007/s40003-020-00516-w

[17] Javadinejad S, Mariwan RDMHH, Hamah A, *et al*. Analysis of Gray Water Recycling by Reuse of Industrial Waste Water for Agricultural and Irrigation Purposes. Journal of Geographical Research, 2020, **3**(2): 1-5.
https://doi.org/10.30564/jgr.v3i2.2056

[18] Javadinejad S, Dara R and Jafary F. Impacts of Extreme Events on Water Availability. Annals of Geographical Studies, 2019, **2**(3): 16-24.

[19] Javadinejad S and Jafary RDF. Gray Water Measurement and Feasibility of Retrieval Using Innova-tive Technology and Application in Water Resources Management in Isfahan-Iran. Journal of Geographical Research, 2020, **3**(2): 1-9.
https://doi.org/10.30564/jgr.v3i2.1997

[20] Javadinejad S, Eslamian S and Ostad-Ali-Askari K. Investigation of monthly and seasonal changes of methane gas with respect to climate change using satellite data. Applied Water Science, 2019, **9**(8): 180.
https://doi.org/10.1007/s13201-019-1067-9

[21] Javadinejad S, Ostad-Ali-Askari K and Eslamian S. Application of Multi-Index Decision Analysis to Management Scenarios Considering Climate Change Prediction in the Zayandeh Rud River Basin. Water Conservation Science and Engineering, 2019, **4**(1): 53-70.
https://doi.org/10.1007/s41101-019-00068-3

[22] Javadinejad S, Dara R and Jafary F. Taking Urgent Actions to Combat Climate Change Impacts. Annals of Geographical Studies, 2019, **2**(4): 1-13.
https://doi.org/10.6084/m9.figshare.10315508

[23] Javadinejad S, Eslamian S, Ostad-Ali-Askari K, *et al*. Embankments. In: Bobrowsky P., Marker B. (eds) Encyclopedia of Engineering Geology. Encyclopedia of Earth Sciences Series. Springer, Cham, 2018.
https://doi.org/10.1007/978-3-319-12127-7_105-1

[24] Javadinejad S, Ostad-Ali-Askari K and Jafary F. Using simulation model to determine the regulation and to optimize the quantity of chlorine injection in water distribution networks. Modeling Earth Systems and Environment, 2019, **5**(3): 1015-1023.
https://doi.org/10.1007/s40808-019-00587-x

[25] Javadinejad S, Eslamian S and Askari K. The analysis of the most important climatic parameters affecting performance of crop variability in a changing climate. International Journal of Hydrology Science and Technology, 2021, **11**(1): 1.
https://doi.org/10.1504/IJHST.2021.112651

[26] Javadinejad S, Dara R and Jafary F. Evaluation of hydro-meteorological drought indices for character-izing historical and future droughts and their impact on groundwater. Resources Environment and Information Engineering, 2020, **2**(1): 71-83.
https://doi.org/10.25082/REIE.2020.01.003

[27] Javadinejad S. The 2008 Morpeth Flood: Continuous Simulation Model for the Wansbeck Catchment. Ebook, Grin publication, 2011.

[28] Mirramazani SM, Javadinejad S, Eslamian S, *et al*. The Origin of River Sediments, The Associated Dust and Climate Change. Journal of Flood Risk Management, 2017, **8**(2): 149-172.
https://doi.org/10.1007/978-3-319-12127-7_105-1

[29] Mirramazani SM, Javadinejad S, Eslamian S, *et al*. A Feasibility Study of Urban Green Space Design in the Form of Smart Arid Landscaping with Rainwater Harvesting. American Journal of Engineering and Applied Sciences, 2018, **201**: 1-9.
https://doi.org/10.3844/ajeassp.201.1-9

[30] Javadinejad S, Dara R and Jafary F. Modelling groundwater level fluctuation in an Indian coastal aquifer. Water SA, 2020, **46**(4): 665-671.
https://doi.org/10.17159/wsa/2020.v46.i4.9081

[31] Javadinejad S, Dara R and Jafary F. Investigation of the effect of climate change on heat waves. Resources Environment and Information Engineering, 2020, **2**(1): 54-60.
https://doi.org/10.25082/REIE.2020.01.001

[32]   Javadinejad S, Dara R and Jafary F. Examining the association between dust and sediment and evaluating the impact of climate change on dust and providing adaptation. Resources Environment and Information Engineering, 2020, **2**(1): 61-70.
https://doi.org/10.25082/REIE.2020.01.002

[33]   Javadinejad S, Dara R, Jafary F, *et al*. Climate change management strategies to handle and cope with extreme weather and climate events. Journal of Geographical Research, 2020, **3**(4): 1-7.
https://doi.org/10.30564/jgr.v3i4.2324

[34]   Javadinejad S, Dara R and Jafary F. How groundwater level can predict under the effect of climate change by using artificial neural networks of NARX. Resources Environment and Information Engineering, 2020, **2**(1): 90-99.
https://doi.org/10.25082/REIE.2020.01.005

[35]   Javadinejad S, Hannah DH, Krause SK, *et al*. The Impacts of Climate Change on Energy-Water Systems and Economic Analysisthe Impacts of Climate Change on Energy-Water Systems and Economic Analysis. The Iraqi Geological Journal, 2020, **53**(2F): 1-17.
https://doi.org/10.46717/igj.53.2F.1Ms-2020-12-24

[36]   Javadinejad S, Hannah D, Krause S, *et al*. Building socio-hydrological resilience "improving capacity for building a socio hydrological system resilience". Safety in Extreme Environments, 2020, **2**(3): 205-218.
https://doi.org/10.1007/s42797-020-00024-8

[37]   Javadinejad S, Dara R, Jafary F, *et al*. A Review on Homogeneity across Hydrological Regions. Biogeneric Science and Research, 2021, **7**(4): 1-13.
https://doi.org/10.46718/JBGSR.2021.07.000173

[38]   Dara R, Jirjees S, Fatah K, *et al*. Climatic Parameters Analysis of Koysinjaq Meteorological Station, Kurdistan Region, Northern Iraq, 2021. Iraqi Geological Journal, **54**(1A): 99-109
https://doi.org/10.46717/igj.54.1A.9Ms-2021-01-30

[39]   Javadinejad S, Dara R and Jafary F. Droughts and the Impacts of Dry Spells in North of Iraq. Research in Ecology, 2021, **3**(1): 59-69.
https://doi.org/10.30564/re.v3i1.2865

[40]   Javadinejad S, Dara R and Jafary F. Climate change simulation and impacts on extreme events of rainfall and storm water in the Zayandeh Rud Catchment. Resources Environment and Information Engineering, 2021, **3**(1): 100-110.
https://doi.org/10.25082/REIE.2021.01.001

[41]   Javadinejad S, Rebwar D and Forough J. Examining the Association Between Dust and Sediment and Evaluating the Impact of Climate Change on Dust and Providing Adaptation. Resources Environment and Information Engineering, 2020, **2**(1): 61-70.
https://doi.org/10.25082/REIE.2020.01.002

[42]   Safieh J, Rebwar D and Hamed MH. Investigation of water quality in wet and dry seasons under climate change. Ukrainian Journal of Ecology, 2020, **10**(5): 94-104.
https://doi.org/10.15421/2020_212

[43]   Javadinejad S, Dara R and Jafary F. Investigation of the effect of climate change on heat waves. Resources Environment and Information Engineering, 2020, **2**(1):54-60.
https://doi.org/10.25082/REIE.2020.01.001

[44]   Javadinejad S, Dara R, Jafary F, *et al*. Modeling the Effects of Climate Change on Probability of Maximum Rainfall and On Variations in Storm Water in the Zayandeh Rud River. Biogeneric Science and Research, 2021, **7**(4): 1-9.
https://doi.org/10.46718/JBGSR.2021.07.000174

[45]   Bogner K, Liechti K and Zappa M. Error Correcting and Combining Multi-model Flood Forecasting Systems. In Advances in Hydroinformatics (pp. 569-578). Springer, Singapore, 2018.
https://doi.org/10.1007/978-981-10-7218-5_40

[46]   Kauffeldt A, Wetterhall F, Pappenberger F, *et al*. Technical review of large-scale hydrological models for implementation in operational flood forecasting schemes on continental level. Environmental Modelling & Software, 2016, **75**: 68-76.
https://doi.org/10.1016/j.envsoft.2015.09.009

[47]   Alvarez-Garreton C, Ryu D, Western AW, *et al*. The impacts of assimilating satellite soil moisture into a rainfall-runoff model in a semi-arid catchment. Journal of hydrology, 2014, **519**: 2763-2774.
https://doi.org/10.1016/j.jhydrol.2014.07.041

[48]   Revilla-Romero B, Beck HE, Burek P, *et al*. Filling the gaps: Calibrating a rainfall-runoff model using satellite-derived surface water extent. Remote Sensing of Environment, 2015, **171**: 118-131.
https://doi.org/10.1016/j.rse.2015.10.022

[49]   Taormina R and Chau KW. Data-driven input variable selection for rainfall-runoff modeling using binary-coded particle swarm optimization and extreme learning machines. Journal of Hydrology, 2015, **529**: 1617-1632.
https://doi.org/10.1016/j.jhydrol.2015.08.022

[50]   Chang FJ, Chiang YM and Ho YH. Multistepahead flood forecasts by neurofuzzy networks with effective rainfall-runoff patterns. Journal of Flood Risk Management, 2015, **8**(3): 224-236.
https://doi.org/10.1111/jfr3.12089

[51]   Reynolds JE, Halldin S, Xu CY, *et al*. Sub-daily runoff predictions using parameters calibrated on the basis of data with a daily temporal resolution. Journal of Hydrology, 2017, **550**: 399-411.
https://doi.org/10.1016/j.jhydrol.2017.05.012

[52] Meng S, Xie X and Liang S. Assimilation of soil moisture and streamflow observations to improve flood forecasting with considering runoff routing lags. Journal of hydrology, 2017, **550**: 568-579. https://doi.org/10.1016/j.jhydrol.2017.05.024

[53] Liu J, Wang J, Pan S, *et al*. A real-time flood forecasting system with dual updating of the NWP rainfall and the river flow. Natural Hazards, 2015, **77**(2): 1161-1182. https://doi.org/10.1007/s11069-015-1643-8

[54] Ciabatta L, Brocca L, Massari C, *et al*. Rainfall-runoff modelling by using SM2RAIN-derived and state-of-the-art satellite rainfall products over Italy. International Journal of Applied Earth Observation and Geoinformation, 2016, **48**: 163-173. https://doi.org/10.1016/j.jag.2015.10.004